2026 Volume: 02 Issue: 07 www.ijrpa.com ISSN 2456-9995 Review Article

International Journal Research Publication Analysis

Page: 01-12

EVALUATION OF LASER GYROSCOPE PERFORMANCE IN UAV ATTITUDE ESTIMATION UNDER ERROR CONDITIONS

***Hoanh Tran Gia**

Master, Faculty of Aeronautical Engineering, Air Defense - Air Force Academy, Hanoi, Vietnam.

Article Received: 30 May 2026
Article Revised: 19 June 2026
Published on: 08 July 2026

***Corresponding Author: Hoanh Tran Gia**
Master, Faculty of Aeronautical Engineering, Air Defense - Air Force Academy, Hanoi, Vietnam.

DOI: https://doi-doi.org/101555/ijrpa.8713

ABSTRACT

This paper presents a comprehensive evaluation of the performance of Ring Laser Gyroscopes (RLG) within Inertial Navigation Systems (INS) for Unmanned Aerial Vehicles (UAVs) under various operational error conditions. Given the stringent accuracy requirements for UAV attitude estimation in dynamic environments, RLGs are selected for their high stability and wide dynamic range. This study focuses on analyzing RLG performance degradation due to primary error sources, including bias drift, white noise, and mechanical vibration-induced errors. Through mathematical modeling and experimental testing on a UAV platform, the research evaluates the capability of estimation filters (such as EKF and UKF) to maintain precision when integrating noisy RLG data. The results demonstrate that accurate modeling of RLG errors is a prerequisite for optimizing compensation algorithms, thereby enhancing the reliability and attitude stability of UAVs in challenging real-world scenarios.

KEYWORD: Ring Laser Gyroscope (RLG); Attitude Estimation; UAV; Inertial Navigation System (INS); Error Modeling; Extended Kalman Filter (EKF).

INTRODUCTION

In recent years, the rapid advancement of Unmanned Aerial Vehicle (UAV) technology has unlocked numerous critical applications, ranging from security surveillance and terrain mapping to autonomous logistics. To execute these missions autonomously, precise attitude estimation (roll, pitch, and yaw) is a core requirement, for which the integrated Inertial Navigation System (INS) is an indispensable component.

Among inertial sensors, the Ring Laser Gyroscope (RLG) has emerged as a superior solution due to its measurement principle based on the Sagnac effect, offering high precision, rapid startup time, and greater resilience to environmental changes compared to traditional MEMS sensors. However, in real-world UAV operational environments, RLGs remain susceptible to various latent error sources, such as sensor bias drift, measurement noise, and high-frequency vibration effects from motors. If not effectively modeled and compensated for, these errors accumulate rapidly during integration, leading to significant inaccuracies in attitude estimation and potential destabilization of the flight control system.

While extensive research exists regarding RLG applications in aerospace, evaluating their performance specifically under the fluctuating operating conditions of UAVs—characterized by lightweight structures and high-vibration profiles—remains an open challenge. This paper aims to bridge this gap by: (1) Deeply analyzing RLG error characteristics within the UAV environment; (2) Developing mathematical models that accurately reflect these error conditions; and (3) Assessing the effectiveness of adaptive filtering algorithms in maintaining attitude precision when such errors occur. The findings of this research provide a vital technical foundation for the design and refinement of next-generation UAV navigation systems in 2026.

METHOD AND MATERIAL

Working Principle of the Laser Gyroscope

The laser gyroscope is engineered based on the motion properties of matter particles. It can be utilized as a sensitive element in instruments such as angular rate sensors and angular position sensors.

Particles utilized as gyroscopic elements can include electrons and atomic nuclei, owing to their orbital and spin moments. Coherent photon streams consisting of particles with such moments can also be employed in these instruments.

Below, we examine the operating principle, range of applications, and sources of noise in the laser gyroscope. The working principle of the laser gyroscope is based on the effect whereby the time taken for an electromagnetic wave to traverse a rotating closed loop differs from the time taken for it to traverse the same loop when it is stationary.

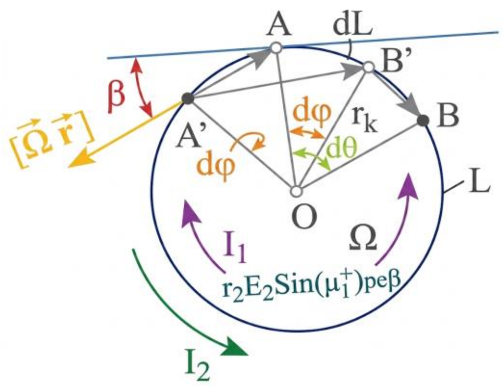

Figure 1. Path of laser beams along the circumference of a closed-loop circuit L.

Assuming that electromagnetic waves I_1 and I_2 travel in opposite directions along the circumference of the loop L (Figure 1). When the loop is stationary, the time taken for the electromagnetic wave to complete the loop L is: $t_1 = t_2 = \frac{L}{C}$

where C is the speed of the electromagnetic wave, approximately 3×10^8 m/s. If the loop rotates around point O with an angular velocity Ω, the dynamic distance between points A and B on the circumference will change ($AB = dL$).

Indeed, for wave I_2, point A will move backward after a time $t = \frac{dL}{C}$, corresponding to a phase lag angle of: $d\varphi = \Omega\frac{dL}{C}$ (1)

In this case, the length BA' will be: $BA' = dL + r_K d\varphi\cos\beta$ (2)

where: r_K is the radius of the loop;

β is the angle between the tangent of the loop in the direction of the tangential velocity component and the chord AA'.

Furthermore: $dL = r_K\frac{d\theta}{\cos\beta}$ (3)

Therefore: $BA' = r_K\frac{d\theta}{\cos\beta} + r_K^2\Omega\frac{d\theta}{C}$ (4)

For wave I_1, the path displacement is shortened to: $BB' = r_K\frac{d\theta}{\cos\beta} - r_K^2\Omega\frac{d\theta}{C}$

Consequently, the optical path difference between the counter-propagating waves is defined as: $\Delta L = BA' - BB' = 2r_K^2\Omega\frac{d\theta}{C}$

When traversing the entire circumference of the loop, the difference in the path lengths traveled by the two waves is: $\Delta L = \dfrac{4\Omega S}{C}$ (5)

where S is the area of the loop.

The relative change in the loop's circumference due to rotation causes the counter-propagating waves to experience a relative phase delay τ, defined by the formula: $\tau = \dfrac{\Delta L}{C} = \dfrac{4\Omega S}{C^2}$ (6)

The phase lag of the two waves (with initial frequency f_0 traveling in the loop per unit time) is determined by the formula: $\Delta\varphi = \dfrac{4\Omega S f_0}{C^2}$ (7)

where f_0 is the frequency of wave propagation in the loop (the number of closed-loop cycles per unit time).

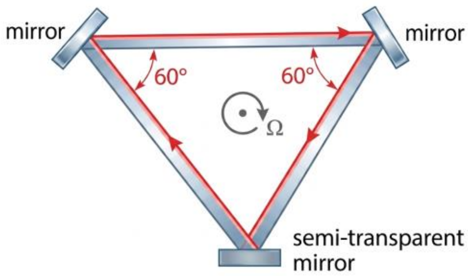

Figure 2. Triangular resonance cavity.

In the event that the loop acts as a resonator with laser frequency, the change in the relative circumference during rotation leads to a change in the resonant frequencies f_1, f_2 of the electromagnetic waves propagating in the resonator in opposite directions. In many studies, it has been determined that the difference between these frequencies is: $\Delta f = \dfrac{8\pi\Omega S}{\lambda L} = k\Omega$ (8)

where λ is the mean wavelength, defined by the expression: $\lambda = \dfrac{4\pi C}{f_1 + f_2}$

k is the scale factor.

For example, for a ring laser operating at a wavelength $\lambda = 0.6\ \mu\text{m}$ with an equilateral triangular resonator (Figure 2) having a side length of $13.2\ \text{cm}$, the frequency difference Δf is approximately $30\ \text{Hz}$ when the angular velocity is $10^o / \text{h}$.

Thus, by determining the frequency difference Δf, we can inversely calculate the angular velocity Ω of the aircraft on which the laser gyroscope is mounted. However, to obtain information regarding the angular velocity Ω, we must first determine the value of Δf.

To determine the Δf (the frequency difference between the two waves), we must employ the heterodyne method.

Based on the property that light waves with different frequencies correspond to different angles of refraction when passing through a prism, this principle is observable in nature, such as when white sunlight passes through a cloud or water droplets, resulting in dispersion and the formation of a rainbow. Consequently, if the laser beams I_1 and I_2 pass through a beam combiner and a prism, they will deviate by an angle ξ. This angle contains information regarding the frequency discrepancy between I_1 and I_2, and thus, information regarding the angular velocity Ω.

To determine the deviation angle ξ (which carries information about the frequency difference Δf and angular velocity Ω according to expression (8)), the interference property of light waves is applied (Figure 3).

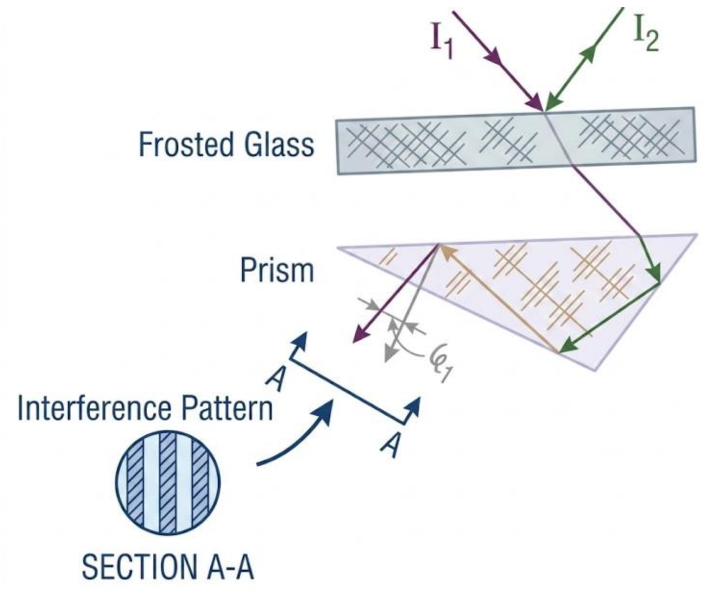

Figure 3. Interference of light waves in a laser gyroscope.

After passing through the prism, the laser beams form an interference pattern of bright and dark fringes on the cross-section A-B. The position of this interference pattern depends on the phase difference between waves I_1 and I_2. Assuming the intensities of I_1 and I_2 are equal and the deviation angle of the beams after the prism is $\xi = \Omega$ (the angular velocity of the resonator ring), the light intensity distribution across the cross-section is determined by the expression:

$$I = I_0\left[1+\cos\left(2\pi\xi/\lambda+2\pi\Delta ft+\varphi_\Phi\right)\right] \quad (9)$$

Where φ_Φ is the initial phase shift (at time $t = t_0$).

From expression (9), it can be seen that if $\Delta f \neq 0$, the bright fringes on the cross-section A-A will shift positions with a frequency of $2\pi\Delta f$. If $\Delta f = 0$, meaning the resonator ring is not rotating, the interference pattern on the cross-section A-A will remain stationary. Thus, the velocity of the shifting light and dark fringes on the interference cross-section reflects the rotation speed of the resonator ring.

The interference image on the cross-section A-A only appears when this cross-section satisfies the spatial conditions of the beams. This means the distance from the cross-section A-A to the prism depends on the natural frequency of the wave, the prism angle, the shape of the resonator ring, and other factors.

For a laser with a wavelength of $\lambda = 0.63\ \mu\text{m}$ and a prism with an angle of $\vartheta = 15''$, the distance between the bright and dark fringes on the interference cross-section is approximately $3\ \text{mm}$. When the photodetector has a size smaller than $3\ \text{mm}$, it can detect the velocity of the moving light and dark fringes on the interference cross-section. If the signals from this photodetector are sent to a counter that tracks the number of times N the bright fringes pass over the photosensitive element per unit of time, this index N carries information about the phase shift between the two signals I_1 and I_2. In other words, when linearity conditions are maintained, these signals are proportional to the angular velocity of the resonator ring (Ω).

Therefore, by mounting resonator rings with counter-propagating electromagnetic beams on a UAV, aligned perpendicular to the UAV's axes of symmetry, the angular velocity of the UAV around these axes can be measured by counting the frequency of bright fringe appearances per unit of time.

Using a single photodetector has the limitation of being unable to determine the direction of rotation. This drawback is easily overcome by utilizing two photodetectors placed at a distance equal to one-quarter of the interference fringe spacing. The placement of these photodetectors is designed to generate signals with a phase shift of 90°. This resolution provides a logical signal that allows for the determination of the resonator ring's direction of rotation (the UAV's angular velocity). If the signal resolution time is Δt, then from expression (8), multiplying both sides by Δt, we obtain:

$$\begin{aligned} \Delta f \Delta t &= \frac{4S}{\lambda L} \cdot 2\pi\Omega\Delta t \\ N_H &= \frac{4S}{\lambda L} Q = N\Delta t \end{aligned} \qquad (10)$$

Where:

N_H is the number of times the bright fringes pass over the photosensitive element during the time interval Δt.

Q is the rotation angle of the resonator during the same time interval.

Thus, based on the difference in the counts N_H from the resonator, the sign of the fringes counted by the two detectors indicates the direction of rotation of the laser resonator.

From expression (10), we observe that the value of N_H depends solely on the final rotation angle of the laser gyroscope (resonator); it is independent of changes in rotation speed. This indicates that, unlike mechanical gyroscopes, laser gyroscopes do not sense acceleration.

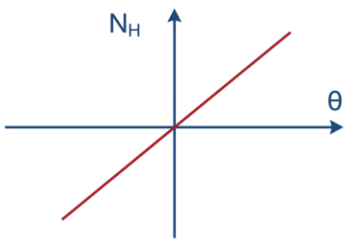

Figure 4. Dependency of N_H on the rotation angle of the laser gyroscope.

If the physical dimensions of the photodetectors are known, the measurement accuracy of the laser gyroscope can be determined. For a laser gyroscope with an equilateral triangular resonator featuring a side length of 13 cm and a laser wavelength of $\lambda = 0.63\ \mu$m, the measurement accuracy is approximately $2''$. This level of accuracy is only attainable in an ideal laser gyroscope, whose characteristics are illustrated in Figure 4.

To measure the rotation angle of a UAV along its axes of symmetry, the analysis of expression (8) is applied. The result of this integration is represented by expression (10), which allows for the determination of the magnitude of the rotation angle. However, to determine the sign of the rotation angle, a logical calculation similar to that used for determining the sign of the angular velocity must be employed. The rotation angle value of the UAV can also be calculated directly by integrating the angular velocity in both magnitude and sign.

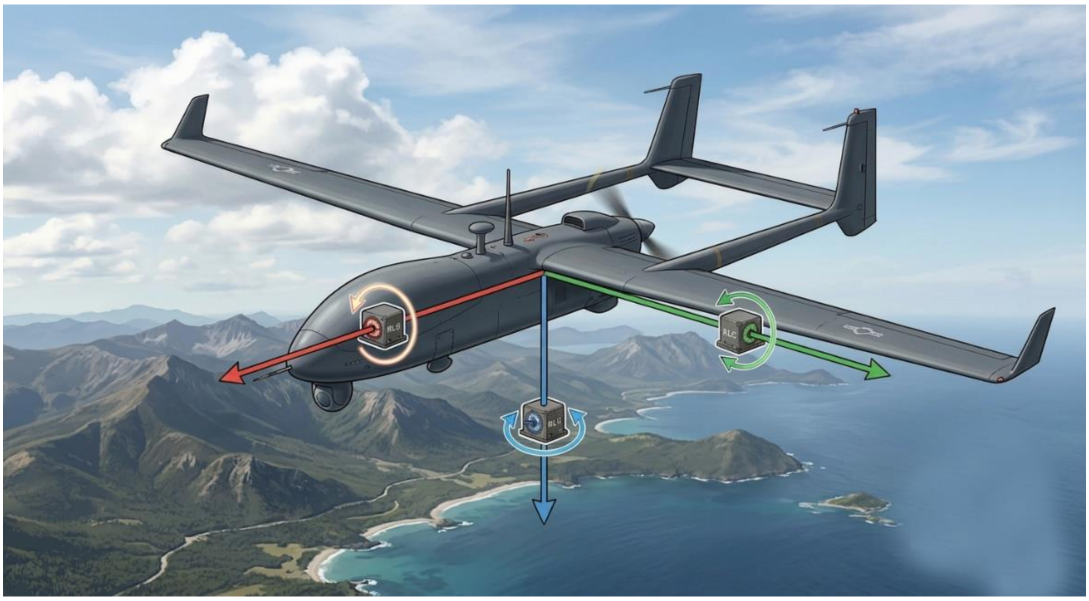

Figure 5. Measurement principle of the laser gyroscope on a fixed-wing UAV.

Simulation of the Laser Gyroscope Using the Sagnac Effect

Figure 6 and Figure 7 illustrate the results obtained from simulating the measurement of the roll and pitch angles of a UAV while the interferometer is in a stationary state. Statistical analysis methods, including the calculation of the mean value and standard deviation, are employed to determine the sensitivity and accuracy of the sensor in detecting minute rotational movements.

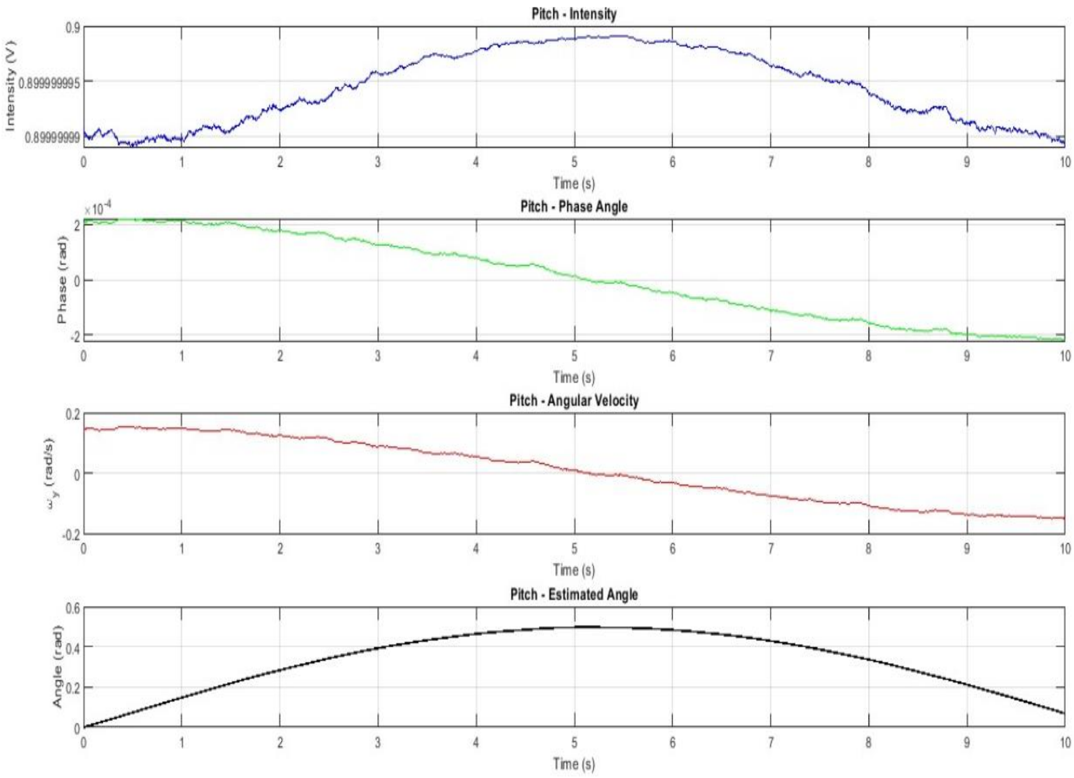

Figure 6. Pitch angle measurement results.

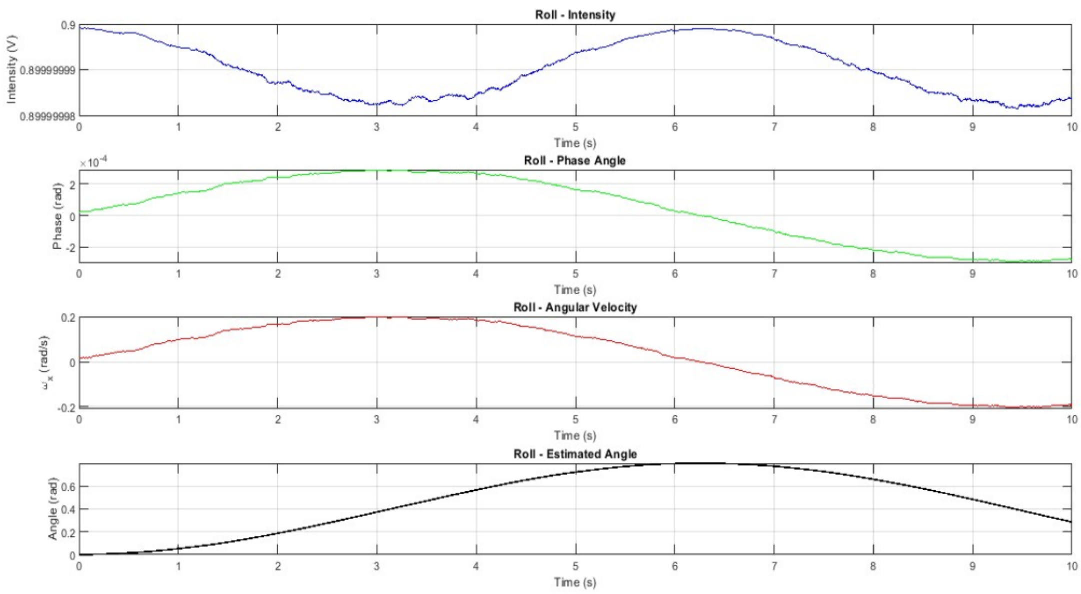

Figure 7. Roll angle measurement results.

Through a systematic data analysis process in MATLAB, the effectiveness of the interferometer in measuring the roll and pitch angles of the UAV is evaluated. Subsequently, various signal processing techniques and mathematical formulations are applied to extract relevant information concerning intensity, phase angle, and angular velocity.

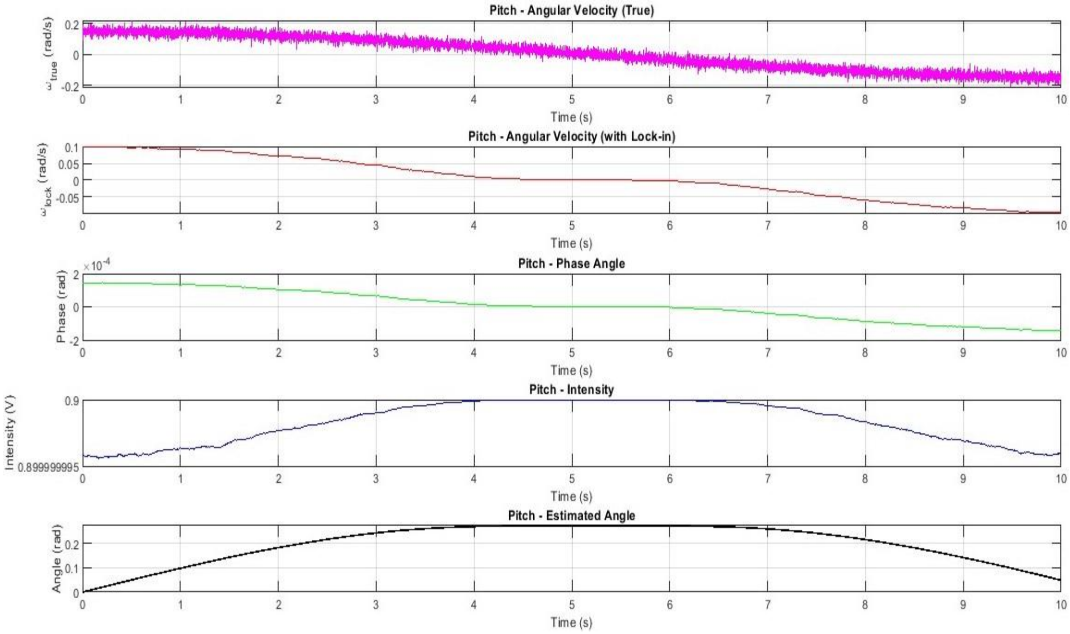

Figure 8. Pitch angle measurement results under lock-in phenomenon.

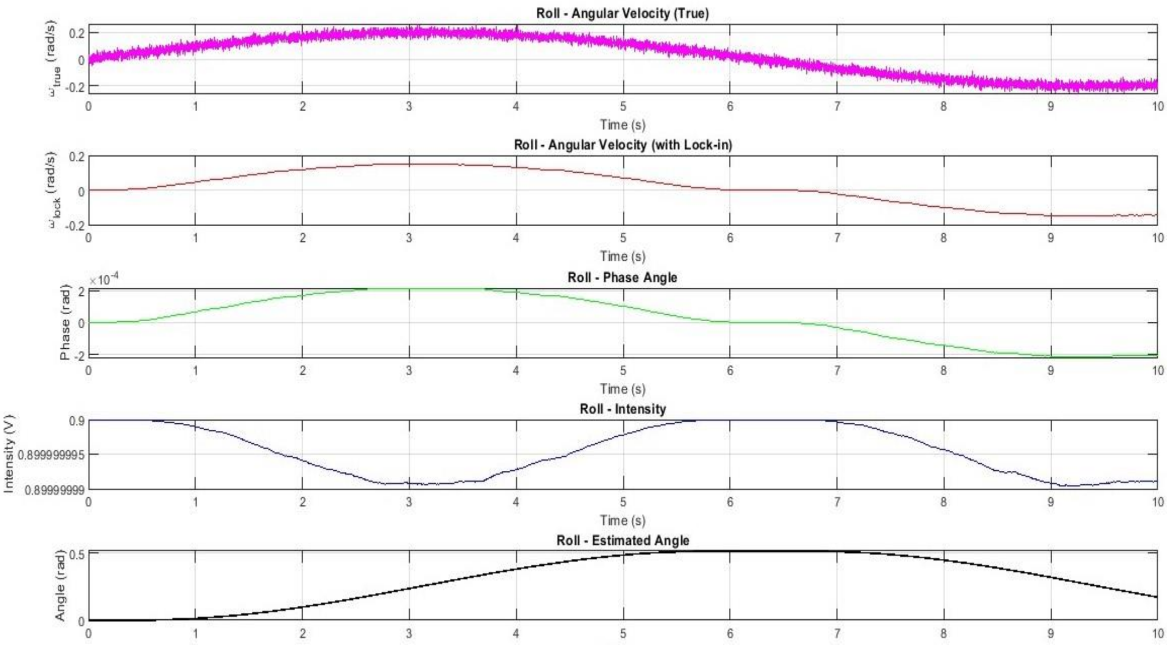

Figure 9. Roll angle measurement results under lock-in phenomenon.

Figures 8 and 9 demonstrate the measurement outcomes when the interferometer oscillates at low frequencies, revealing the significant impact of the lock-in phenomenon on both pitch and roll angle estimations. In these regimes, the non-linear "dead zone" characteristic leads to systematic errors in the output, as the sensor fails to detect small angular rates effectively.

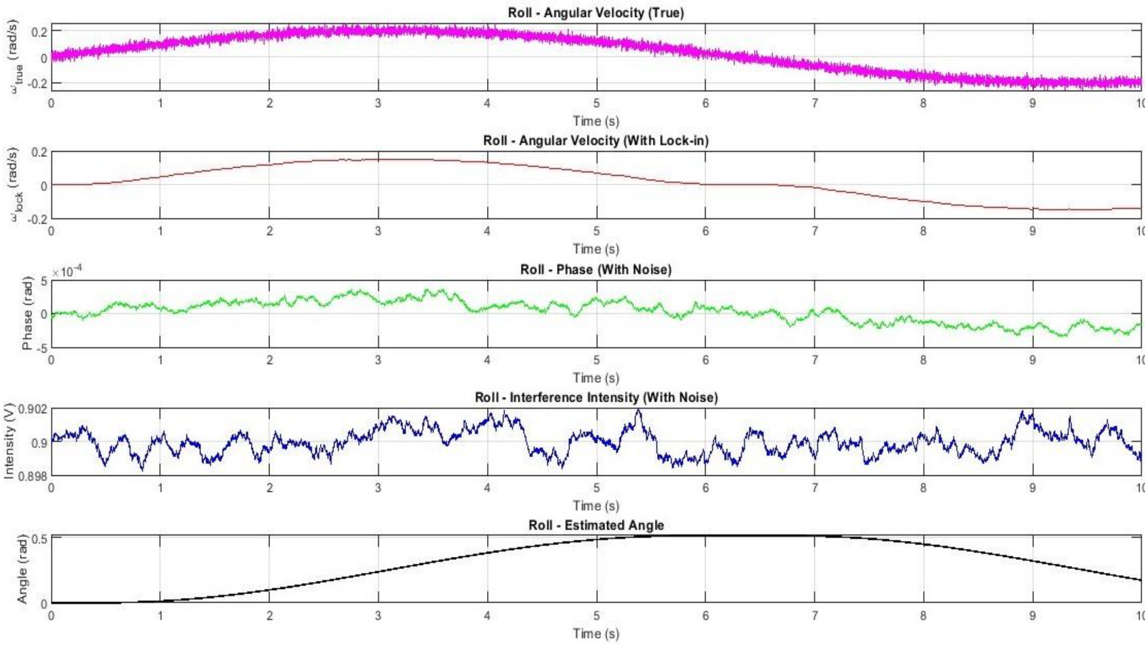

Figure 10. Roll angle measurement results under noisy conditions.

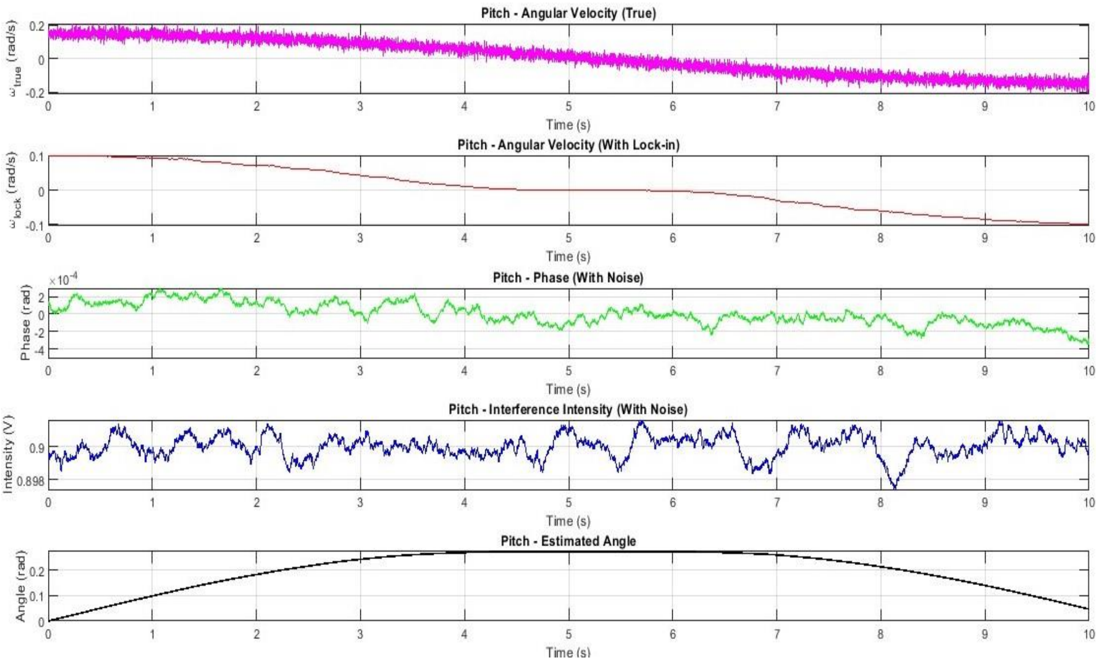

Figure 11. Pitch angle measurement results under noisy conditions.

Initially, the acquired signal contains significant noise, which is subsequently smoothed using the movmean function in MATLAB. Following this, the intensity is utilized to compute the phase angle, from which the angular velocity is derived. Finally, the angular velocity is integrated to calculate the UAV's roll and pitch angles.

CONCLUSION

Throughout this study, we have systematically presented and analyzed the operating principle of the Ring Laser Gyroscope (RLG), grounded in the Sagnac effect-the fundamental phenomenon that enables the detection and measurement of rotation via the phase difference between two counter-propagating laser beams within a common resonant cavity. A thorough understanding of this theoretical foundation serves as the vital prerequisite for the simulation and implementation of RLGs in UAV roll and pitch measurement systems.

The research results demonstrate that the Ring Laser Gyroscope possesses significant advantages over traditional inertial sensors, such as high precision, long-term stability, and the capability to operate in rigorous environmental conditions. These attributes provide a robust basis for integrating RLGs into modern Inertial Navigation Systems (INS) and Attitude and Heading Reference Systems (AHRS). Looking ahead, the synergy between RLG technology and advanced filtering and calibration algorithms promises to further enhance reliability and practical application in the autonomous guidance and control of UAVs.

REFERENCES

1. Aronowitz, Frederick: The Laser Gyro, in: Laser Applications vol. 1; Academic Press, New York 1971, S. 133-200.
2. W. Luhs: The Laser Gyro; MEOS GmbH, Januar 2000.
3. Meschede, Dieter: Optics, Light and Lasers; Wiley-VCH Verlag, Weinheim 2004.
4. Shimoda, Koichi: Introduction to Laser Physics; Springer Verlag, Berlin Heidelberg 1984.